Tribol Lett (2015) 60:11
DOI 10.1007/s11249-015-0578-2

ORIGINAL PAPER

Tribological Properties of Limonene Bisphosphonates

Girma Biresaw[1] · **Grigor B. Bantchev**[1]

Received: 13 July 2015 / Accepted: 18 August 2015 / Published online: 9 September 2015
© Springer Science+Business Media New York (outside the USA) 2015

Abstract Limonene was chemically modified by reacting it with dialkyl phosphites of varying alkyl structures under inert atmosphere in the presence of free radical initiators. The reaction gave a mixture of mono- and di-adduct products and was optimized to produce only the di-adduct product limonene bisphosphonate by forcing both limonene double bonds to react completely. The product mixture was carefully characterized using a combination of gas chromatography–mass spectroscopy, infrared spectroscopy, and nuclear magnetic resonance spectroscopy (^{1}H, ^{13}C, ^{31}P). The bisphosphonates were investigated for their physical and tribological properties. The alkyl bisphosphonates displayed density and viscosity that was a function of the alkyl structure (methyl, ethyl, *n*-butyl) and much higher than the values for the unreacted limonene. They also displayed improved oxidation stability but lower viscosity index and solubility in polyalphaolefin (PAO6) and high-oleic sunflower oil (HOSuO) base oils. Tribological characterization of the neat modified oils on a four-ball tribometer showed improved extreme-pressure weld point by all three di-adducts and improved anti-wear coefficient of friction (COF) and wear scar diameter (WSD) by the *n*-butyl di-adduct only. The limonene bisphosphonates also displayed improved COF and WSD as additives in PAO6 and HOSuO base oils at low concentrations. The effects of chemical modifications on physical and tribological properties can be explained in terms of increased polarity of the modified products, insertion of heavy atoms (from PO_3) into the limonene structure, and complete absence of unsaturation in the modified products.

Keywords Limonene · Bisphosphonates · Chemical modification · Synthesis · Polarity · Four-ball tribometer · Anti-wear · Extreme pressure · Weld point · Coefficient of friction · Wear scar diameter · PDSC · Onset temperature · Peak temperature · GC–MS · NMR · FTIR

1 Introduction

Biobased lubricants are those formulated from ingredients derived from natural products as opposed to most lubricants currently in the market, which are petroleum-based [1]. Biobased lubricants are being developed because they provide a number of benefits over petroleum-based lubricants [2]. Biobased lubricants can be based on renewable farm products and thus provide sustainable economic development to rural and farm communities. Biobased lubricants are environmentally friendly because they are biodegradable and cause minimal harm to the environment, wildlife, fish, and humans during production, use, and disposal. Another major environmental benefit of biobased lubricants is their effect on global warming. Unlike petroleum-based lubricants which are net emitters of greenhouse gases, farm-based production of biobased lubricant ingredients can remove greenhouse gases from the atmosphere. Thus, biobased lubricants can be net negative

Mention of trade names or commercial products in this publication is solely for the purpose of providing specific information and does not imply recommendation or endorsement by the US Department of Agriculture. USDA is an equal opportunity provider and employer.

✉ Girma Biresaw
girma.biresaw@ars.usda.gov

[1] Bio-Oils Research Unit, National Center for Agricultural Utilization Research, Agricultural Research Service, United States Department of Agriculture, 1815 N. University Street, Peoria, IL 61604, USA

emitters of greenhouse gases and, hence, help fight global warming [3].

Early biobased lubricant development was based on commodity vegetable oils such as soybean oil and their derivatives [1]. Such lubricants displayed a number of beneficial tribological properties including high viscosity index (VI), low volatility, low boundary friction, enhanced extreme-pressure (EP) additive performance, and low traction coefficient [4–8]. Such oils also displayed a number of misgivings such as poor oxidation stability, poor cold flow property, poor hydrolytic stability, and poor bioresistance relative to petroleum-based oils [1, 4, 9, 10]. In order to remedy these and other performance issues with commodity oil biobased lubricants, their development was expanded in many directions including to application of vegetable oils from new crops [11, 12] as well as from genetically modified crops [6]. Other areas being aggressively explored for the development of new biobased base oils and additives with improved properties include the modification of the structures of vegetable oils and their derivatives (fatty acids, fatty esters, etc.) by chemical [13–15], thermal [16, 17], and enzymatic [18] methods.

Recently, the raw material base for the development of biobased lubricants has expanded beyond vegetable oils and derivatives, to plant sugars and algal oils, which are converted into biobased lubricant ingredients via microbial fermentations [19]. Another non-vegetable oil plant-based raw material with potential for use in biobased lubricant development is limonene [20, 21]. In this paper, we describe our investigation into the chemical modification of limonene and the evaluation of the new products for use as biobased EP and/or anti-wear (AW) [22] lubricant additives.

Limonene, also known as dipentene, is a natural product widely found in many plants as a constituent of "essential oils" [20, 21]. As shown in Table 1, the amount of limonene in essential oils varies from trace quantities to up to 95 % [20].

Commercial limonene is a by-product of the citrus industry obtained from the processing of fruits such as oranges, lemons, lime, tangerine, mandarins, and grapefruits [23, 24]. Major citrus oil producing countries include: Argentina, Brazil, Italy, Mexico, South Africa, Spain, Turkey, and the USA [24].

Limonene is a C10 hydrocarbon with cyclic branching, two double bonds, and a chiral carbon in its structure (Fig. 1) [20, 21]. The compound is relatively inert at mild temperatures which allows it to be used without further modification in various medical and industrial applications including in: bioadhesive tablets [25]; solvent-cleaning compositions [26–33]; lubricant formulations [34–36]; surface protection/anti-corrosion formulations [37]; topical surface treatment/surface protection formulations (polishing, disinfecting, degreasing, deodorizing, lubricating, cleaning) [38]. Various applications have also been reported for limonene and terpenes that were chemically modified by the introduction of halogens, sulfur, phosphorous, and combinations thereof into their structures. Examples include: halogenated terpenes as germicides and insecticides [39]; sulfurized terpenes in lubricating oils with improved antioxidant and anti-corrosion and improved seal compatibility properties [40–48]; chlorinated and sulfurized limonene as an EP additive [49]; terpenes containing sulfur and phosphorous as lubricating oil additives with improved antioxidant, anti-corrosion, sludge inhibition, and wear resistance properties [50–57].

Table 1 Maximum limonene composition of selected "essential oils" [20]

Essential oil	Max [limonene (%)]
Lavender oil	1
Bay leaf oil	1
Lavender spike oil	1.2
Palmarosa oil	1.7
Pimento berry oil	1.8
Thyme oil	1.8
Lavandin oil	2
Coriander seed oil	2.5
Eucalyptus oil	2.7
Thuja oil	3.3
Tagetes oil	3.9
Galbanum oil	4
Citronella oil	4
Nutmeg oil	5.8
Cornmint oil	7.1
Sage oil	7.1
Juniper oil	8.7
Citronella oil	9
Orange flower oil	11.6
Rosemary oil	14.1
Black pepper oil	18
Spearmint oil	21.4
Bergamot oil	42
Lime oil	45
Dutch caraway oil	47
Lemon oil	66
Grapefruit oil	93
Bitter orange oil	94
Orange oil	95

2 Experimental

2.1 Materials

R (+) Limonene (97 %, 98 % enantiomeric excess) and 2,2′-azobis(2-methylpropionitrile), 98 % (AIBN) were

Fig. 1 Structure of limonene

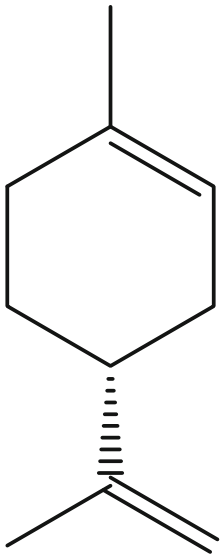

(R)-(+)-limonene

obtained from Sigma-Aldrich (St. Louis, MO). Dimethyl phosphite (98 %) and diethyl phosphite (96 %) were from Alfa Aesar (Ward Hill, MA). Di-*n*-butyl phosphite (96 %), dilauroyl peroxide (LPO), 99 %, and di-*tert*-butyl peroxide (BPO), 99 %, were from Acros Organics (Geel, Belgium). Ethyl acetate (HPLC grade) was from EMD Chemicals, Inc. (Gibbstown, NJ). Hexanes (HPLC grade), isopropyl alcohol (99.9 %), Na_2SO_4, $MgSO_4$, and $NaHCO_3$ were from Thermo Fisher Scientific, Inc. (Pittsburgh, PA). Extra dry N_2 was from ILMO Products Company (Jacksonville, IL). High-oleic sunflower oil (81 % oleic acid) was purchased from Columbus Foods Company (Des Plaines, IL). Polyalphaolefin with a viscosity of 6 cSt at 100 °C (PAO6), sold under the trade name Durasyn 166, was a free sample from Ineos Oligomers (League City, TX). All chemicals were used as supplied. Steel balls used in four-ball tribological experiments were obtained from Falex Corporation (Aurora, IL) and were cleaned prior to use by consecutive 10-min sonications in isopropyl alcohol and hexane solvents. The steel balls have the following specifications: material, chrome steel alloy made from AISI E52100 standard steel; hardness, 64–66 Rc; diameter, 12.7 mm; finish, grade 25 extra polish.

2.2 Synthesis, Purification and Analysis

2.2.1 General Synthesis Procedure

The reactions were carried out in a round-bottom flask with magnetic stirrer and nitrogen-filled balloon to keep an inert atmosphere. BPO, which has a half-life of 10 h at 125 °C [58], was used as the radical initiator. The reaction temperature (125 °C) was maintained, using a heating mantle with a proportional/integral/derivative (PID) controller (Ace Glass, Inc., Vineland, NJ) and a thermocouple (OMEGA Engineering, Inc., Stamford, CT). The progress of the reaction was monitored using GC–MS and was stopped when the limonene double bonds had completely reacted. The reaction product was a mixture of isomers, which had similar MS spectra and very few unique fragments. Because of this, only generalized MS spectra are given, with abundances listed as a range observed for the different isomers. The products were also characterized using NMR and FTIR.

2.2.2 Analytical Instruments

NMR NMR spectra were obtained in $CDCl_3$ on a Bruker Avance 500 NMR spectrometer (Billerica, MA) operating at 500 MHz for ^{1}H, 202 MHz for ^{31}P, and 126 MHz for ^{13}C, using a 5-mm broad-band observe probe. Chemical shifts for ^{1}H and ^{13}C are reported in parts per million (ppm) from tetramethylsilane calculated from the lock signal; the chemical shifts of ^{31}P are reported in ppm from 85 % H_3PO_4 calculated from the lock signal. The NMR signals for the product mixtures did not have many distinct signals, except for the alkoxy groups bonded to the P. The other signals were combinations of many weak signals, due to the material being a mixture of similar isomers, and also from ^{31}P splitting. The observed ^{31}P (36–31 ppm) signals were typical for phosphonate moieties ($C–P(=O)(OR)_2$).

GC–MS The GC–MS was from Agilent Technologies (Santa Clara, CA) with a model 7890A GC-oven and a model 5975C MS triple axis detector with inert XL EI/CI MSD. MS in the electron impact (EI) mode was used. The conditions were: mass range 34–720 amu, 22 sampling rate, and electron multiplier 0 V relative. The instrument was equipped with a SPB-1 column (30 m × 0.25 mm × 0.25 μm) from Supelco, Inc. (Bellefonte, PA). The inlet conditions were 250 °C with a He flow rate of 1 mL/min. The oven program was a ramp of 4 °C/min from 100 to 300 °C, followed by a 12-min hold at 310 °C. In a typical procedure, 40 μL of the reaction mixture were diluted in 1 mL ethyl acetate, and 0.2 μL of the diluted solution were injected in the GC–MS.

FTIR The instrument was a model 3100 FTIR spectrometer (Varian, Inc., Randolph, MA), equipped with a Ge multipass attenuated total reflectance (ATR) crystal from Pike Technologies (Madison, WI). Sixty-four repeat scans were averaged over a range of 600–5000 cm^{-1} at a spectral resolution of 4 cm^{-1}.

2.2.3 Synthesis and Characterization of Di-n-butyl Phosphite Di-adducts of Limonene

Under nitrogen atmosphere, 84.04 g (0.618 mol) limonene and 438 g (2.258 mol) di-*n*-butyl phosphite were placed in

a flask with a nitrogen-filled balloon and a magnetic stirring bar to which 10.22 g (0.070 mol) of BPO initiator were added at the beginning of the reaction. The reaction was stopped when the GC–MS showed disappearance of the limonene (23 h). The product mixture was then stripped of excess di-*n*-butyl phosphite and some of the side products by Kugelrohr distillation (110 Pa, 80 °C for 3 h, followed by 150 Pa, 115 °C for 5 h). The product contained some acidic di-*n*-butyl phosphate, which was either present in the original di-*n*-butyl phosphite or was formed during the synthesis by the oxidation of the di-*n*-butyl phosphite with the peroxide initiator. The product was dissolved in a mixture of 40 g EtOAc/200 g hexane mixture; sequentially washed with saturated solutions of $NaHCO_3$ and Na_2SO_4; and dried with anhydrous Na_2SO_4. Hexane and EtOAc were removed by distillation (330 Pa, 60 °C for 1 h, followed by 50 Pa, 80 °C for 3.5 h) to give 288 g of purified product (89 % yield). The product was characterized by FTIR, NMR, and GC–MS.

IR-ATR, cm^{-1}:

2959 (s), 2874 (m), 1464 (m), 1381 (w), 1238 (s), 1067 (s), 1024 (s), 976 (s), 903 (w), 835 (w).

NMR:

^{1}H, ppm: 4.08–3.84 (8.0H, $POCH_2$-), 2.19–1.93 (1.5H), 1.93–1.62 (4.4H), 1.62–1.51 (9.2H), 1.51–1.39 (2.2H), 1.39–1.28 (8.8H), 1.14–0.91 (7.0H), 0.91–0.81 (12.6H, $PO(CH_2)_3CH_3$).

^{13}C{H}, ppm: 65.3–64.6 ($POCH_2$-), 64.4–64.6 ($POCH_2$-), 45.0–42.5, 41.7–41.4, 39.5–38.9, 38.5, 38.2, 37.4, 37.1, 36.5-36.1, 33.7, 33.3, 33.0, 32.7-32.5 ($POCH_2CH_2$-), 32.1, 31.7, 30.5–30.0, 29.4–29.1, 28.6, 28.2, 28.0, 27.7, 27.4–27.3, 21.4, 20.2, 19.8, 18.8, 18.7 ($PO(CH_2)_2CH_2$-), 17.3, 17.2, 17.1–17.0, 15.1, 14.2, 13.8, 13.5 ($PO(CH_2)_3CH_3$).

^{31}P{H}, ppm: 35.14–35.03 (0.1P), 33.49–33.41 (0.1P), 33.38–33.31 (0.1P), 33.05–32.91 (1.1P), 32.91–32.85 (1.0P), 32.85–32.73 (1.0P), 32.73–32.66 (0.8P), 32.66–32.54 (0.3P), 32.42–32.22 (1.2P), 31.80–31.65 (0.2P).

GC–MS:

GC–MS revealed 94.3 % di-adduct product (8 peaks with MW = 524 and retention times from 45.2 to 49.0 min.), 3.1 % mono-adduct peak (MW = 330, retention time 27.0 min), and 2.5 % others (tri-*n*-butyl phosphate and other peaks).

The di-*n*-butyl phosphite mono-adduct peak had the following main fragments (*m/z* (abundance %, proposed fragment composition)): 330 (88, M^+), 315 (18, $[M\text{-}CH_3]^+$), 274 (10, $[M\text{-}C_4H_8]^+$), 259 (23), 219 (29, $C_{10}H_{17}P(OH)_3]^+$), 218 (28, $C_{10}H_{17}P(O)(OH)_2]^+$), 203 (30), 175 (20), 167 (27), 153 (34), 149 (33), 136 (100, $[M\text{-}(BuO)_2HPO]^+$), 121 (65), 109 (60), 93 (92), 83 (69, $[HP(OH)_3]^+$), 81 (59).

The di-*n*-butyl phosphite di-adducts had the following main fragments: *m/z*(abundance % range, proposed fragment composition): 524 (1–2, $[M]^+$), 509 (3–15, $[M\text{-}CH_3]^+$), 469 (13–23, $[M\text{-}C_4H_7]$), 413 (2–3, $[M\text{-}Bu\text{–}C_4H_8]^+$), 331 (51–100, $[M\text{-}P(O)(OBu)_2]^+$), 317 (58–100, $[M\text{-}CH_2\text{-}P(O)(OBu)_2]^+$), 289 (21–74, $[M\text{-}C_3H_6P(O)(OBu)_2]^+$), 283 (0–36), 235 (19–35, $[C_3H_6P(O)(OBu)_2]^+$), 219 (18–66, $[C_2H_2P(O)(OBu)_2]^+$), 205 (10–20), 177 (10–23), 153 (11–19), 151 (7–19), 137 (17–43), 135 (11–18), 123 (36–67, $[C_3H_6P(O)(OH)_2]^+$), 97 (18–32, $[CH_3P(OH)_3]^+$), 83 (11–41, $[HP(OH)_3]^+$).

2.2.4 Synthesis and Characterization of Diethyl Phosphite Di-adducts of Limonene

To a closed round-bottom flask equipped with a magnetic stirrer, N_2-filled balloon and thermocouple were added 64.27 g (0.473 mol) limonene, 374.83 g (2.72 mol) $(EtO)_2HPO$, and 4.44 g (0.0304 mol) BPO initiator. The mixture was heated with stirring at 125 °C for 22 h, at which time GC–MS indicated a complete reaction of the double bonds, and the reaction was stopped. Excess diethyl phosphite was removed by distillation under reduced pressure (80 °C and 50 Pa for 2 h, followed by 100 °C and 50 Pa for 3 h). The stripped product was dissolved in 200 mL hexane and washed with 200 mL saturated $NaHCO_3$ aqueous solution. This gave a three-phase mixture (aqueous phase/aqueous and hexane phase/hexane phase). The aqueous phase was discarded, and more water from the middle phase was removed by the addition of $MgSO_4$. The remaining non-aqueous phase was stripped of solvents by distillation under reduced pressure (80 °C and 50 Pa) and resulted in 185.3 g (95 % yield) of purified product. The product was characterized by FTIR, NMR, and GC–MS.

IR-ATR, cm^{-1}:

2974 (m), 2930 (m), 2897 (m), 1439 (w), 1387 (w), 1238 (m), 1165 (w), 1078 (w), 1051 (s), 1026 (s), 951 (s), 785 (w).

NMR:

^{1}H, ppm: 4.11–3.90 (8.0H, $POCH_2$-), 2.13–2.02 (0.8H), 2.02–1.91 (0.8H), 1.91–1.71 (2.9H), 1.71–1.48 (3.3H), 1.48–1.29 (2.5H), 1.28–1.15 (13.0H, $POCH_2CH_3$), 1.13–0.83 (7.5H), 0.82–0.72 (0.3H).

^{13}C{H}, ppm: 61.4–60.9 ($POCH_2$-), 60.7–60.5, 44.8–43.0, 42.7, 41.6, 39.4–38.8, 38.5, 37.4, 37.1, 36.5–36.2, 33.7, 33.3, 32.9, 32.0, 31.7, 30.5, 30.1, 30.0, 29.4, 29.0, 28.4, 27.8, 27.3, 21.4, 20.2, 20.1, 19.9, 19.8, 17.3, 17.1, 16.5–16.4 ($POCH_2CH_3$), 14.1.

^{31}P{H}, ppm: 35.96–35.89 (0.1P), 35.12–35.05 (0.1P), 33.49–33.44 (0.1P), 33.44–33.40 (0.1P), 32.86–32.76 (1.8P), 32.75–32.70 (1.0P), 32.68–32.57 (0.8P), 32.56–32.49 (0.0P), 32.45–32.19 (0.9P), 31.89–31.85 (0.1P), 31.82–31.74 (0.1P).

GC–MS:

GC–MS showed 2.3 % mono-adduct and 97.7 % di-adducts (9 or 10 peaks, some of them not very well resolved). Other compounds were also present in trace amounts.

GC–MS of the mono-adduct: *m/z* (abundance %, proposed fragment composition): 274 (74, $[M]^+$), 259 (43, $[M\text{-}CH_3]^+$), 245 (7, $[M\text{-}CH_3]^+$), 231 (23), 205 (22), 192 (10), 177 (9), 165 (56, $[C_2H_4P(O)(OEt)_2]^+$), 152 (63, $[CH_2P(O)(OEt)_2]^+$), 149 (18), 139 (44), 136 (72, $[C_{10}H_{16}]^+$), 125 (18), 121 (85), 111 (39), 109 (42), 93 (100), 91 (45), 81 (63), 79 (35), 67 (29).

GC–MS of the di-adducts: *m/z* (abundance % range, proposed fragment composition): 412 (1–2, $[M]^+$), 397 (5–22, $[M\text{-}CH_3]^+$), 275 (46–100, $[M\text{-}P(O)(OEt)_2]^+$), 261 (52–100, $[M\text{-}CH_2P(O)(OEt)_2]^+$), 247 (3–13, $[M\text{-}C_2H_4P(O)(OEt)_2]^+$), 233 (28–83, $[M\text{-}C_3H_6P(O)(OEt)_2]^+$), 219 (4–10,), 205 (4–5,), 179 (21–37, $[C_3H_6P(O)(OEt)_2]^+$), 165 (5–7, $[C_2H_4P(O)(OEt)_2]^+$), 138 (11–26, $[P(O)(OEt)_2]^+$), 123 (33–47, $[C_3H_6P(O)(OH)_2]^+$) 109 (9–17), 95 (15–28,), 93 (9–14), 81 (16–34,), 65 (5–12).

2.2.5 Synthesis and Characterization of Dimethyl Phosphite Di-adducts of Limonene

To a round-bottom flask (1 L) equipped with a N_2-filled balloon and a magnetic stirrer were added dimethyl phosphite (410.38 g, 3.73 mol), limonene (83.97 g, 0.617 mol), and BPO initiator 6.33 g (43.4 mmol). The two-phase reaction mixture was stirred vigorously and heated, and then a single phase was obtained when the temperature exceeded 55 °C. The mixture was maintained at 125 °C for 18 h at which time GC–MS showed complete reaction of all limonene double bonds, and the heat was removed. Excess phosphite was removed from the product mixture with Kugelrohr distillation (80 °C, 90 Pa for 2.5 h; followed by 1.7 h at 100 °C) to which 100 mL of EtOAc was added. The mixture was then extracted three times with 150 mL of saturated aq. $NaHCO_3$, followed by three washes with 100 mL of 1 M aq. Na_2SO_4. The organic phase was separated and treated with anhydrous Na_2SO_4 to expel more water, and dried over anhydrous Na_2SO_4. The organic phase was stripped of the solvent under reduced pressure (310 Pa and 60 °C for 2 h, followed 100 °C and 160 Pa for 1 h), filtered through a Buchner filter (#50) to remove particulates and collected 186.6 g (85 % yield) of purified product. The product was characterized by FTIR, NMR, and GC–MS.

IR-ATR, cm^{-1}:

2951 (m), 2849 (w), 16.38 (w), 1454 (w), 1231 (m), 1049 (s), 1028 (s), 812 (m).

NMR:

^{1}H, ppm: 3.65–3.45 (12.0H, P-OCH_3), 3.44–3.32 (0.4H), 2.14–1.97 (0.8H), 1.97–1.79 (1.0H), 1.79–1.61 (2.8H), 1.61–1.40 (3.4H), 1.40–1.28 (2.0H), 1.28–1.02 (1.9H), 1.02–0.89 (3.7H), 0.89–0.74 (3.8H), 0.74–0.65 (0.2H).

^{13}C{H}, ppm: 52.3–51.7 (P-OCH_3), 51.5–51.3, 43.9–42.9, 42.6–42.4, 42.1, 42.0, 41.0, 40.9, 39.1, 39.0, 38.6, 38.5, 38.1, 37.8, 37.0, 36.8, 36.3–35.9, 34.2, 33.5, 33.3, 32.7, 32.5, 31.8, 31.7, 30.2, 30.0, 29.5, 29.4, 28.9, 28.5, 28.4, 28.3, 28.3, 27.3, 27.2, 27.1, 24.2, 23.3, 21.2, 20.0, 19.9, 17.1, 17.0, 16.8, 14.1.

^{31}P{H}, ppm: 38.02–37.97 (0.0P), 37.67–37.59 (0.0P), 35.90–35.85 (0.1P), 35.85–35.80 (0.1P), 35.42–35.29 (0.6P), 35.29–35.16 (1.0P), 35.18–35.02 (0.7P), 35.02–34.93 (0.1P), 34.89–34.69 (0.6P), 34.25–34.16 (0.1P), 34.16–34.04 (0.1P).

GC–MS:

GC–MS showed one mono-adduct (1.3 %) and 10 di-adducts (98.7 %) peaks. Peaks of other compounds were also observed in trace quantities.

GC–MS of the mono-adduct: *m/z* (abundance %, proposed fragment composition): 246 (30, $[M]^+$), 231 (64, $[M\text{-}CH_3]^+$), 203 (24), 177 (27), 164 (11), 137 (89), 136 (78), 124 (60), 121 (84), 111 (35), 110 (37, $[HP(O)(OCH_3)_2]^+$), 93 (100), 91 (31), 79 (58), 77 (26), 69 (15).

GC–MS of the di-adducts: *m/z* (abundance % range, proposed fragment composition): 356 (1–2, $[M]^+$), 341 (2–22, $[M\text{-}CH_3]^+$), 301 (0–12), 247 (37–100, $[M\text{-}P(O)(OCH_3)_2]^+$), 233 (52–100, $[M\text{-}CH_2P(O)(OCH_3)_2]^+$), 219 (1–10), 205 (30–100, $[M\text{-}C_3H_6P(O)(OCH_3)_2]^+$), 192 (1–3), 191 (4–10), 179 (2–17), 165 (7–11), 152 (7–17, $[C_3H_7P(O)(OCH_3)_2]^+$), 151 (29–62, $[C_3H_7P(O)(OCH_3)_2]^+$), 137 (7–21), 124 (28–40, $[CH_3P(O)(OCH_3)_2]^+$), 123 (23–48, $[CH_2P(O)(OCH_3)_2]^+$), 110 (20–49, $[HP(O)(OCH_3)_2]^+$), 109 (20–40, $[P(O)(OCH_3)_2]^+$), 95 (24–54), 93 (18–25), 81 (15–31), 79 (26–46).

2.3 Characterization of Physical and Tribological Properties

Solubility Solubility (% w/w) at room temperature of phosphite di-adducts of limonene, in polyalphaolefin (PAO6) and high-oleic sunflower oil (HOSuO) base oils,

was determined gravimetrically by visual inspection for any changes in oil transparency.

Refractive Index Refractive index as a function of temperature (20–80 °C) was measured on an Abbe Mark II Plus Refractometer (Reichert, Inc., Depew, NY). Data at 100 °C were obtained by extrapolation of measured data at ≤80 °C.

Density, Viscosity, and Viscosity Index (VI) Density and dynamic and kinematic viscosities were measured on a Stabinger SVM3000/G2 viscometer (Anton Paar GmbH, Graz, Austria). VI was calculated from kinematic viscosity and density data at 40 and 100 °C following the procedure outlined in the ASTM D 2270-93 [59].

Pressurized Differential Scanning Calorimetry (PDSC) PDSC tests were conducted on a Q20P pressure differential scanning calorimeter (TA Instruments—Waters LLC, New Castle, DE) fitted with a computer and appropriate software to allow for data acquisition and analysis. All tests were conducted with the cell pressurized with pure oxygen to 500 ± 25 psig in dynamic mode, i.e., with a positive oxygen flow rate of 100 ± 10 mL/min. Details of the test procedure have been given before [60]. Duplicate runs were conducted, and average values of onset temperature (OT) and peak temperatures (PT) are reported.

Four-Ball (4-ball) Tribological Tests Tests were conducted on a model KTR-30L four-ball tribometer equipped with TriboDATA software (Koehler Instrument Company, Bohemia, NY). The specification and detailed description of the instrument hardware and software have been given before [61].

Four-Ball Anti-Wear (AW) Test Four-ball AW tests were conducted according to the ASTM D 4172-94 procedure [62]. The coefficient of friction (COF) from each test was calculated from the corresponding torque and load data according to the ASTM D 5183 procedure [63]. Wear scar diameters, along and across the wear direction of the three balls from each test, were measured on a wear scar measurement system, comprising hardware and ScarView software (Koehler Instrument Company, Inc., Bohemia, NY), and were averaged. Each test lubricant was used in at least two AW measurements, and average COF and wear scar diameter (WSD) values were reported.

Four-Ball Extreme-Pressure (EP) Test A four-ball EP test was conducted according to the ASTM D 2783 procedure [64]. In this procedure, a series of 10 seconds tests are conducted at increasing loads until welding of the four balls is observed. The load at which welding occurred is recorded and reported as the weld point of the lubricant tested. Lubricants with superior EP properties display higher weld points.

2.4 Data Analysis

Data analysis was conducted using IgorPro version 5.0.3.0 software (WaveMetrics, Inc., Lake Oswego, OR).

3 Results and Discussion

3.1 Synthesis

The synthesis of limonene bisphosphonate is illustrated in Scheme 1. The reaction involves free radical addition of the H-P of the dialkyl phosphite (**2a**, **b** or **c**) across one or both double bonds of limonene (**1**). The reaction is conducted under nitrogen atmosphere without solvent and in the presence of a free radical initiator (**5**, **6** or **7**) and excess dialkyl phosphite. The structures of the reactants are summarized in Scheme 1.

The reactions were carried out for 18–24 h at temperatures appropriate for the selected initiator. The reaction produces a mixture of mono- and bisphosphonate products, whose ratio is a function of the reaction conditions. As discussed below, the reaction can be optimized to produce almost only the bisphosphonate (or di-adduct) product mixture.

Isolation of the phosphonate product mixture is achieved first by removing the excess phosphite by distillation. The remaining product mixture is then dissolved in hexanes, and acidic residues are removed by extraction with saturated aqueous $NaHCO_3$ and dried over anhydrous Na_2SO_4. The purified phosphonate product mixture is then isolated by removing the hexanes by distillation.

The mono- and bisphosphonate product mixtures were positively identified using a combination of GC–MS, FTIR, and NMR as described below.

The progress of the reactions and extent of purifications were monitored using GC–MS. Figure 2 shows the total ion count traces for the GC–MS of the partially reacted product mixtures. The crude product mixture contained some peaks of lower molecular weight compounds. These include unreacted dialkyl phosphites, initiator decomposition products, and some side products. The low molecular weight compounds were removed by distillation and subsequent washes. GC–MS also showed that the crude product mixture contained a small fraction of mono-adduct products which did not react further to form the di-adducts. The mono-adducts were somewhat volatile and were partially removed from the final product mixture during the Kugelrohr distillation. The identification of the mono- and di-adduct compounds was accomplished by analyzing the mass spectra. GC–MS showed the presence of several isomers of the mono-adduct and di-adduct products with similar fragmentation patterns. An example of a fragmentation pattern for a di-adduct isomer is given in Fig. 3. We estimate that the product mixture could comprise up to nine mono-adduct and 18 di-adduct stereoisomers. The separation and identification of individual mono- and di-adduct isomers are beyond the scope of this paper.

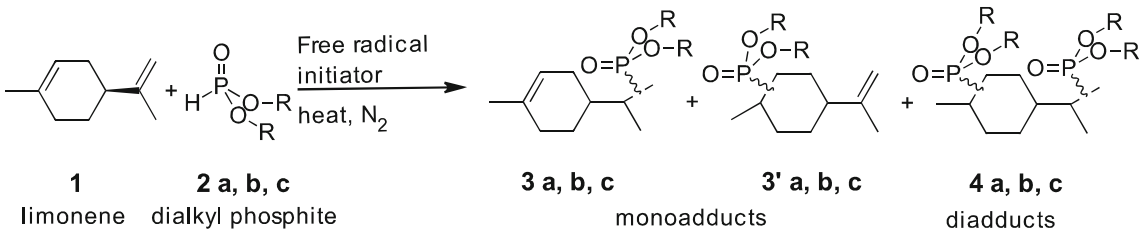

a: R = methyl
b: R = ethyl
c: R = *n*-butyl

Free Radical Initiator:

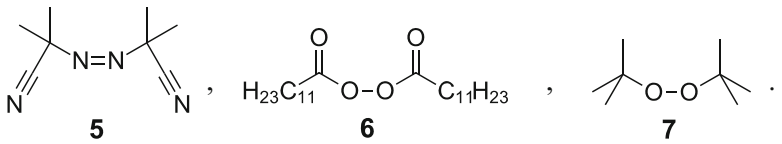

Scheme 1 Generalized scheme for synthesis of limonene phosphonates

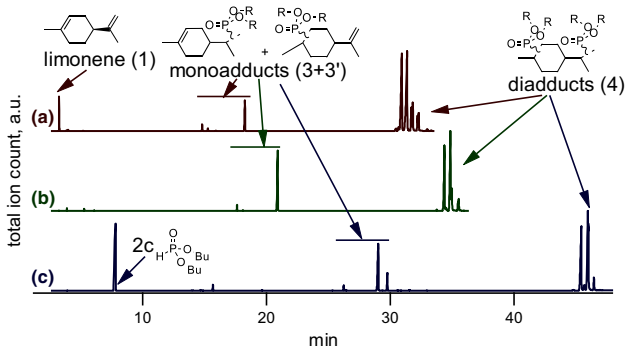

Fig. 2 GC traces of the product mixture containing mono-adduct (**3, 3′**) and di-adduct (**4**) products (see Scheme 1). **a** R = methyl, **b** R = ethyl and **c** R = *n*-butyl

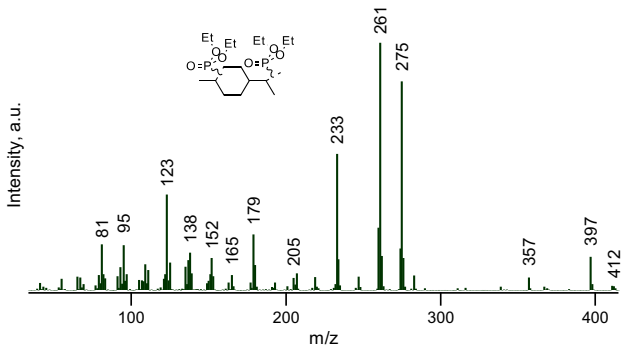

Fig. 3 MS spectrum of the most abundant isomer of product **4b**. Similar MS spectra were obtained for the less abundant isomers of **4b**

The FTIR spectra of the purified product mixture without the mono-adduct product, i.e., with only the bisphosphonate products, are shown in Fig. 4 The spectra show no peaks at ~3100 and ~1650 cm^{-1}, indicating the complete reaction of the limonene double bonds. It also shows strong signals in the region of 850–1250 cm^{-1}, which are typical of compounds containing P=O and P–O–R groups [65].

The ^{1}H and ^{13}C NMR spectra of the di-adduct product mixture without mono-adduct products are shown in Figs. 5 and 6, respectively. The spectra confirm the FTIR results discussed above, i.e., that all the double bonds have reacted by the absence of peaks around 5.5 ppm in ^{1}H NMR (Fig. 5) as well as the peaks at 105–150 ppm in ^{13}C NMR (Fig. 6). In addition, the absence of absorptions in the 6.7–6.8 ppm range of the ^{1}H NMR (Fig. 5),

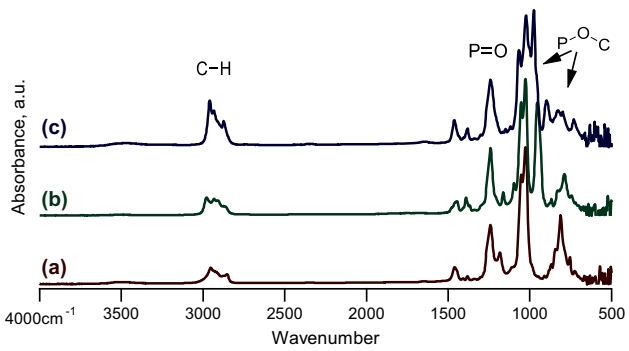

Fig. 4 FTIR spectra of the product mixture containing only di-adduct products (**4**) and none of the mono-adduct products (see Scheme 1). *a* R = methyl, *b* R = ethyl and *c* R = *n*-butyl

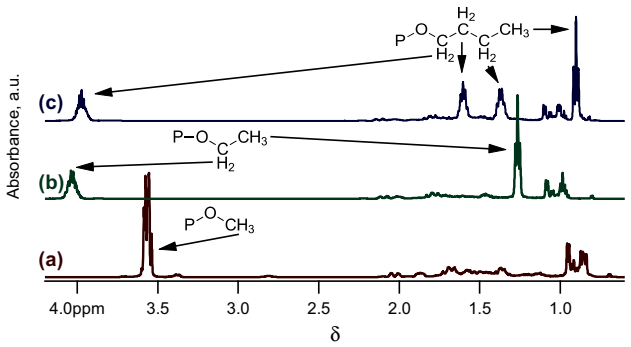

Fig. 5 ^{1}H NMR spectra of the product mixture containing only di-adduct products (**4**) and none of the mono-adduct products (see Scheme 1). *a* R = methyl, *b* R = ethyl and *c* R = *n*-butyl. There are no signals outside the region shown other than the CDCl3 peak at 7.3 ppm

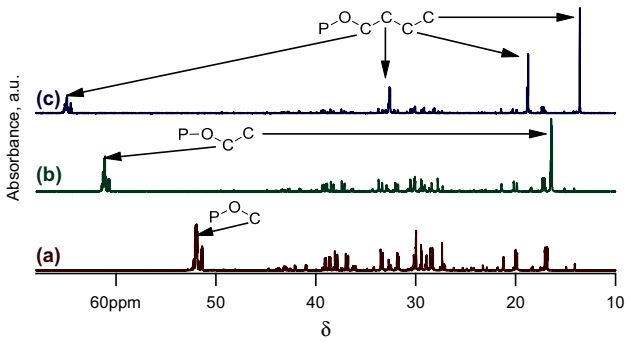

Fig. 6 ^{13}C NMR spectra of the product mixture containing only di-adduct products (**4**) and none of the mono-adduct products (see Scheme 1). *a* R = methyl, *b* R = ethyl and *c* R = *n*-butyl. There are no signals outside the region shown other than the CDCl3 triplet at ~77 ppm

corresponding to H bonded to the P atom, indicates all the unreacted dialkyl phosphite reagent has been completely removed from the product mixture. The most prominent peaks in both the ^{1}H and ^{13}C NMR spectra are those due to the alkoxy groups attached to the P atoms. These peaks appear at 96, 1.56, 1.33, and 0.86 ppm for the *n*-butyl derivative; 4.00 and 1.21 ppm for the ethyl derivative; and 3.55 ppm for the methyl derivative in ^{1}H (Fig. 5), and they appear at 64.9, 32.6, 18.7, and 13.5 ppm for the *n*-butyl derivative; 61.2 and 16.4 ppm for the ethyl derivative; 52.0 ppm for the methyl derivative in ^{13}C NMR (Fig. 6). Rest of the peaks in both ^{1}H and ^{13}C NMR spectra are less pronounced, due to the product being a mixture of isomers, and the splitting effect of the P atoms.

The ^{31}P NMR spectra of the product mixture with only the di-adduct products and without mono-adduct products are shown in Fig. 7. The spectra show peaks only in the 30–40 ppm region, which is consistent with the presence of phosphonates [65–67]. The crude product obtained after distillation of the dialkyl phosphite showed no signals in

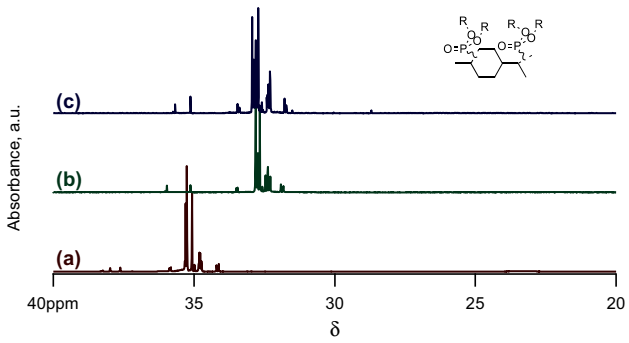

Fig. 7 ^{31}P NMR spectra of the product mixture containing only di-adduct products (**4**) and none of the mono-adduct products (see Scheme 1). *a* R = methyl, *b* R = ethyl and *c* R = *n*-butyl. There are no signals outside the region shown

the region of 6–12 ppm. This indicates that all the unreacted dialkyl phosphite had been removed. Some weak signals were observed in the region of −5 to +5 ppm in the ^{31}P NMR spectra of the crude product mixture. This indicates that some of the dialkyl phosphites were oxidized to phosphates. However, these signals were not observed in the product obtained after washing with saturated aqueous $NaHCO_3$ solution.

Investigations were conducted to determine optimum reaction conditions for maximizing bisphosphonates and minimizing the mono-phosphonates in the product mixture. A series of reactions were conducted in which the following were varied: structure of the alkyl phosphites; structure and concentration of free radical initiators; limonene to phosphite ratio. The relative amount of mono- and bisphosphonate adducts in the product mixture obtained from varying the reaction conditions were monitored.

The result of the investigation is summarized in Table 2. The first three entries of Table 2 show the effect of varying the type of initiator on the composition of the reaction mixture. The only differences in the reaction conditions between these three entries were the initiator type and the reaction temperatures, which were selected to be appropriate for the particular free radical initiator [58]. As seen in Table 2, the proportion of bisphosphonate in the product mixture from di-*n*-butyl phosphite increased in the order: AIBN < LPO < BPO. A similar investigation using diethyl phosphite (entries 4, 5 in Table 2) confirmed the trend and showed an increased proportion of the bisphosphonate product in the order: AIBN < BPO. The data in Table 2 also show that the increased proportion of the bisphosphonate product can be obtained by increasing the dialkyl phosphite to the limonene ratio. This is illustrated in Table 2 by comparing reaction 5 versus 9 for the synthesis with diethyl phosphite, and reactions 3 versus 6 for the synthesis with di-*n*-butyl phosphite.

Table 2 Reaction conditions investigated in phosphonate synthesis optimization

#	Limonene (mmol)	Alkyl phosphite [mmol (molar ratio)][a]	Free radical initiatorb [mmol (molar ratio)][a]	Temp (°C)	Time (h)	Phosphonate product [% (GC)]	
						Mono-	Bis-
1	5.74	*n*-Butyl, 25.3 (2.20)	AIBN, 1.0 (0.087)	65	24	83	12
2	5.74	*n*-Butyl, 25.3 (2.20)	LPO, 1.0 (0.087)	65	24	21	79
3	5.74	*n*-Butyl, 25.3 (2.20)	BPO, 1.0 (0.087)	125	24	3	97
4	12.6	Ethyl, 46.8 (1.86)	AIBN, 0.91 (0.036)	64	24	67	5
5	7.7	Ethyl, 41.2 (2.7)	BPO, 1.2 (0.078)	125	24	8	92
6	618	*n*-Butyl, 2258 (1.83)	BPO, 70 (0.057)	125	23	10	90
7	617	Methyl, 3730 (3.02)	BPO, 43.4 (0.035)	125	18	6	94
8	468	Methyl, 2850 (3.04)	BPO, 31.8 (0.034)	125	21	3	97
9	473	Ethyl, 2720 (2.87)	BPO, 30.4 (0.032)	125	22	2	98

[a] Moles of reagent per mole of limonene double bond

[b] Initiators: AIBN: 2,2′-azobisisobutyronitrile; LPO: dilauroyl peroxide; BPO: di-*tert*-butyl peroxide

3.2 Density, Viscosity, and Refractive Index

Table 3 compares the density, viscosity, VI, and refractive index data of limonene bisphosphonate derivatives with those of limonene. Values at 40, 75, and 100 °C were generated in this work and are compared with available literature data [68]. The data show that conversion of limonene to its bisphosphonate derivatives had a considerable effect on its physical properties.

The density of unmodified limonene at 40 °C is 0.8267 g/mL and increased to >1.01 g/mL for the three bisphosphonate derivatives. The density of the bisphosphonate derivatives was dependent on the structure of the alkoxy group of the phosphonate and increased in the order: *n*-butyl < ethyl < methyl at all temperatures. At ≥75 °C, the density of the *n*-butyl bisphosphonate derivative decreased to below 1.00 g/mL. However, the density of the ethyl and methyl derivatives remained above 1.03 g/mL up to 100 °C.

The increase in the density of the limonene derivatives can be attributed to the insertion of heavier elements (P, O) into the structure of limonene as well as to the increased polarity of the limonene derivatives. The phosphonate structure will make the derivatives polar, thereby introducing stronger intermolecular dipole interactions. The polarity of the structures should increase with decreasing chain length in the order: *n*-butyl < ethyl < methyl, which is similar to the order of increasing density.

As expected, the refractive index of limonene and its derivatives increased with increasing density.

Another major change due to the bisphosphonation of limonene is viscosity, which is an important tribological property. As shown in Table 3, the dynamic viscosity of the *n*-butyl bisphosphonate derivative at 40 °C was almost 100-fold larger than that of limonene, whereas the corresponding value for the methyl derivative was more than 500-fold larger. As with density, viscosity values were a function of the temperature and the structure of the alkoxy substituent of the phosphonate group. Thus, dynamic and kinematic viscosities at all temperatures increased as a function of the alkoxy structure in the order: *n*-butyl < ethyl < methyl.

Among the factors that contribute to the dramatic rise in viscosity is the increased molecular weight of the bisphosphonate derivatives due to the insertion of the two phosphonate groups into the structure of limonene. Also, the branching introduced by the phosphonate groups will cause entanglements that will result in increased viscosity. Finally, intermolecular dipolar interactions of the polar phosphonate groups, which increase with decreasing chain length of the alkoxy substituent, are also a major contributor to the increase in viscosity of the bisphosphonate derivatives of limonene.

Another major property of great interest in tribology is VI. As shown in Table 3, bisphosphonation generally resulted in lowering the VI of limonene. The data in Table 2 also show that the VI value was dependent on the structure of the alkoxy substituent of the phosphonate group and decreased in the order: *n*-butyl > ethyl > methyl. This trend suggests that decreasing chain length results in decreasing of VI. It is not clear whether this is a general trend of lubricating oils, since there are no reports of studies linking branch chain length with VI of lubricating fluids. A similar observation on the effect of carboxylic ester branch chain length on the VI of chemically modified vegetable oils has been reported [69].

3.3 Oxidation Stability

Oxidation stability of limonene and its bisphosphonate derivatives were investigated using PDSC. The method

Table 3 Physical properties of limonene and bisphosphonate derivatives

	Limonene	Limonene bisphosphonates		
		n-Butyl	Ethyl	Methyl
Refractive index[a]				
40 °C	(1.4368)[b]	1.4581	1.4613	1.4717
75 °C		1.4461	1.4486	1.4601
100 °C		1.4369	1.4394	1.4525
Density (g/mL)				
40 °C	0.8267 (0.8290)[b]	1.0172	1.0809	1.1633
75 °C	0.7994	0.9909	1.0536	1.1352
100 °C	0.7794	0.9722	1.0344	1.1154
dVisc (mPa s)				
40 °C	0.68 ± 0.00 (0.722)[b]	64.89 ± 0.01	73.95 ± 0.02	347.94 ± 18.76
75 °C	0.48 ± 0.00	15.96 ± 0.00	16.09 ± 0.00	43.95 ± 1.63
100 °C	0.37 ± 0.00	7.94 ± 0.00	7.78 ± 0.01	17.06 ± 0.52
kVisc (mm^2/s)				
40 °C	0.83 ± 0.00	63.80 ± 0.01	68.41 ± 0.02	299.10 ± 16.20
75 °C	0.60 ± 0.00	16.11 ± 0.00	15.28 ± 0.00	38.71 ± 1.43
100 °C	0.47 ± 0.00	8.17 ± 0.00	7.53 ± 0.01	15.30 ± 0.46
Viscosity Index	96	95	60	5

All data from this work unless noted; standard deviations for RI and Density: 0.0000–0.0002

[a] Data at 100 °C extrapolated from measured values at ≤80 °C

[b] Values in parenthesis are literature data from Ref [68]

measures the temperature at which oxidation begins or reaches a maximum rate when the samples are heated under pressure in pure oxygen. These temperatures are called onset (OT) and peak (PT) temperatures, respectively. Higher OT and PT correspond to higher oxidation stability.

Table 4 compares the OT and PT values of limonene and its bisphosphonate derivatives, along with those of polyalphaolefin (PAO6) and high-oleic sunflower oil (HOSuO) base oils. These two base oils were selected for this study because they have similar viscosity but different polarity [60]. As shown in Table 4, bisphosphonation dramatically improved the OT and PT of limonene above the values reported for HOSuO [60] and close to those measured for PAO6. The latter is well known to be a very thermally stable synthetic base oil [6]. There was no obvious trend of the effect of phosphonate substituent chain length on OT or PT. The data show that the methyl was the most stable, followed by the *n*-butyl, and the ethyl was the worst.

Limonene is expected to display poor thermal stability because it contains numerous reactive allylic protons associated with the two double bonds in its structure (Fig. 1). Bisphosphonation eliminates the double bonds along with the reactive allylic protons, thereby producing a material with highly improved oxidation stability. HOSuO contains fewer double bonds than limonene, which accounts for its higher OT and PT values relative to limonene. However, because of the double bonds, HOSuO still displayed OT and PT values that were much lower than the values for the fully saturated oils (Table 4).

3.4 Solubility

Limonene bisphosphonates have potential applications as lubricant additives with AW, anti-friction and EP properties. In order to be used in such applications, the bisphosphonates have to display sufficient compatibility with and solubility in base oils commonly used in lubricant formulations. Thus, the room-temperature solubility of limonene and its bisphosphonates derivatives in PAO6 and HOSuO were investigated. The results of the investigation are summarized in Table 5. As shown in Table 5, unmodified limonene was miscible with both base oils. However, the solubility of its bisphosphonate derivatives varied depending on their structure as well as the polarity of the base oil. In general, the bisphosphonates were more soluble in HOSuO than in PAO6. This result is consistent with the well-known rule of thumb, "like dissolves like," since the bisphosphonates and HOSuO are more polar compared with PAO6. Further analysis of the solubility data shows that the solubility of the bisphosphonates in PAO6 improved with increasing alkyl chain length (or decreasing polarity) in the order: methyl < ethyl < *n*-butyl. In

Table 4 PDSC onset temperature (OT) and peak temperatures (PT) of limonene and bisphosphonates (°C)

	Limonene	Limonene bisphosphonates				
		n-Butyl	Ethyl	Methyl	PAO6	HOSuO[a]
OT	140.8 ± 1.4	191.5 ± 2.5	183.9 ± 1.9	199.9 ± 1.1	198.6 ± 0.7	187.2 ± 0.6
PT	154.3 ± 2.0	217.8 ± 1.4	210.4 ± 1.4	219.3 ± 0.7	217.7 ± 1.1	200.0 ± 0.2

All data from this work unless noted

[a] Data from Ref. [60]

HOSuO, solubility increased in the order: methyl ~ ethyl < *n*-butyl, indicating a possible mismatch in polarity between the HOSuO base oil and the bisphosphonates (ethyl and methyl) additives.

3.5 Tribological Properties

The tribological properties of limonene bisphosphonate derivatives were investigated as neat and also as additives in PAO6 and HOSuO blends. Investigations were conducted on a four-ball tribometer under AW (ASTM D 4172 procedure [62]; ASTM D 5183 procedure [63]) and EP (ASTM D 2783 procedure) configurations. The AW and EP results of the neat oil investigations are summarized in Table 6, where the data for the bisphosphonates are compared to each other and to the base oils (PAO6 and HOSuO).

Examination of the neat oil EP results in Table 6 shows that bisphosphonates provide weld points of about double (~200 kgf) the reported values [60, 61] for the neat base oils. Among the bisphosphonates, the methyl product gave a higher (260 kgf) weld point than the *n*-butyl or ethyl products. The EP result suggests that neat bisphosphonates provide improved EP properties over the neat base oils, but the improvements were rather small since commercial EP additives provide much higher weld points (>800 kgf) at much lower concentrations (<20 %) [61]. Thus, more work is needed to develop a commercially viable EP additive based on limonene.

Table 5 Room-temperature solubility of limonene and bisphosphonate derivatives in polyalphaolefin (PAO6) and high-oleic sunflower oil (HOSuO) base oils (% w/w)

Base oil	Solubility (% w/w)			
	Limonene	Bisphosphonates		
		n-Butyl	Ethyl	Methyl
PAO6	>50	6.96	4.21	2.15
HOSuO	>50	10.17	7.15	7.06

All data from this work unless noted

The AW test provides two parameters for comparing the performance of the oils: COF and WSD. Examination of the neat AW results in Table 6 shows that the *n*-butyl bisphosphonate product provides the lowest COF and WSD than the ethyl or methyl products. In fact, the COF and WSD values from the *n*-butyl bisphosphonate are comparable or better than the values for the neat HOSuO base oil. On the other hand, the COF and WSD values from the methyl and ethyl bisphosphonate products were much higher than the values for the neat HOSuO or PAO6 base oils.

The results of the AW investigation into the additive properties of limonene bisphosphonate in PAO6 and HOSuO base oils are summarized in Fig. 8. In this investigation, the COF and WSD were measured as a function of limonene bisphosphonate concentrations in each of the base oils. Looking at the COF data first (Fig. 8a), and as mentioned before, neat HOSuO displays a significantly lower COF than neat PAO6. Without exception, the addition of 1 % limonene bisphosphonate to either base oil lowered the COF by an amount that was dependent on the type of bisphosphonate. A further increase in additive concentration to 3 % did not cause a further reduction in COF, but increased it to values above the COF of the neat base oil. A further increase in additive concentration to 5 % produced no change or a slight increase in COF. The only exception to this observation was the ethyl bisphosphonate product in HOSuO, which showed a further decrease in the COF at 3 % and no change at 5 %.

Inspection of the WSD data (Fig. 8b) shows different trends for the two base oils. To begin with, the neat HOSuO produces a much lower WSD than the neat PAO6. Incorporation of any of the three bisphosphonate additives into HOSuO resulted in a lower WSD to about 0.4 mm. The further addition of bisphosphonate to HOSuO resulted in a slight increase or no change in WSD. The outcome was different when additives were blended into PAO6. The addition of the first 1 % of the bisphosphonate resulted in an increase, decrease, or no change of the WSD, depending on the alkyl structure of the bisphosphonate material. However, for all three bisphosphonate materials, a further increase in the concentration in PAO6 above 1 % resulted in an increase of the WSD (Fig. 8b).

Table 6 Anti-wear (ASTM D4172) and extreme-pressure (ASTM D 2783) properties of neat limonene bisphosphonate

	Limonene bisphosphonate			PAO6	HOSuO
	n-Butyl	Ethyl	Methyl		
Anti-wear[a]					
COF	0.069 ± 0.002	0.126 ± 0.004	0.117 ± 0.016	0.089 ± 0.006	0.066 ± 0.005
WSD (mm)	0.523 ± 0.005	0.940 ± 0.003	1.024 ± 0.001	0.923 ± 0.060	0.668 ± 0.004
Extreme pressure[b]					
Weld point (kgf)	200	200	260	120[c]	120[d]

All data from this work unless noted

[a] ASTM D 4172 [62]; ASTM D 5183 [63]

[b] ASTM D 2783 [64]

[c] Data from Ref [61]

[d] Data from Ref [60]

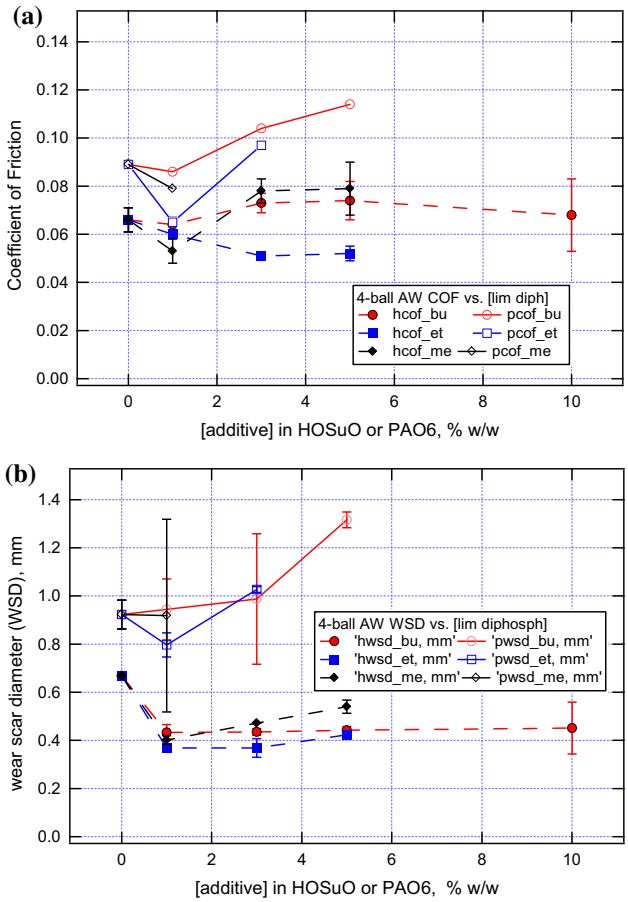

Fig. 8 Limonene bisphosphonate in PAO6 (*open*) or HOSuO (*filled symbols*) versus four-ball anti-wear: COF (**a**); WSD (**b**)

3.6 Structure–Property Considerations

Phosphonylation of limonene resulted in new structures with increased density and viscosity as shown in Table 3. The increases were also dependent on the structure of the alkyl substituents in the phosphite reactant (Scheme 1). In general, the density of limonene increased from below 0.83 g/mL to greater than 1.16 g/mL, and can be attributed to the introduction of heavier elements (from PO_3) into its structure as a result of the chemical modification.

The phosphonate also increases the polarity, which will increase the density due to the increased intermolecular interaction in the modified molecule. The density of modified limonenes increases in the order: *n*-butyl < ethyl < methyl, which follows the expected trend of increasing polarity. Polarity is also responsible for the observed 20- to 40-fold increase in viscosity after phosphonylation. As with density, the viscosity of modified limonene increases in the order: *n*-butyl < ethyl < methyl, which follows the trend of polarity increase with alkyl structure. Table 3 also shows that chemical modification lowered the VI of limonene. As shown in Table 3, VI decreased in the order: limonene ≥ *n*-butyl > ethyl > methyl. This trend is the reverse of the polarity trend for the structures and suggests that VI increases with decreasing polarity. This observation is consistent with what is known on the effect of polarity on the VI of vegetable oils [4] and modified vegetable oils [69]. For example, vegetable oils that contain the polar hydroxyl groups in their structures display a much lower VI (e.g., castor, VI = 87; lesquerella, VI = 124) than those that do not (e.g., soybean, VI = 227; canola, VI = 215, etc.) [4]. In the case of modified vegetable oils, the VI of esterified polyhydroxy milkweed oil was found to be dependent on the structure of the anhydride used in the esterification [69]. The VI increased in the order: polyhydroxy (not esterified) < acetate < butyrate < valerate, which is the order of increasing non-polarity of the oils [69].

Another property that is also affected by changes in polarity due to chemical modification is solubility in polyalphaolefin (PAO6) and high-oleic sunflower (HOSuO) base oils (Table 5). While limonene is miscible with both base oils, the bisphosphonates displayed limited

solubility (≤10 %) in HOSuO, and even lower in PAO6 (≤7 %), which is less polar than HOSuO. The solubility of the bisphosphonates in both base oils decreased with increasing polarity of the alkyl groups. Thus, solubility and non-polarity decreased in the order: *n*-butyl > ethyl > methyl.

Another major structural change due to phosphonylation of limonene is the loss of unsaturation (Scheme 1). Addition to the two double bonds in limonene resulted in the loss of several allylic protons which are known to be prone to oxidation. PDSC analysis of limonene before and after modification (Table 4) clearly shows improvements in OT and PT after chemical modification. In fact, the chemically modified phosphonates displayed oxidation stability comparable to PAO6 (Table 4), which is well known to possess excellent oxidation stability [6].

Phosphorous is one of a handful of elements known to provide beneficial tribochemical properties to base oils and additives [22]. In the present case, phosphonylation produced minor improvements in EP and mixed results in AW properties (Table 6). The chemically modified neat oils showed similar EP properties that were slightly higher than the base oils (PAO6 and HOSuO). AW properties were generally worse than the values for the base oils except for the neat *n*-butyl product, which showed similar COF and better WSD than the neat HOSuO. It is not clear why the methyl and ethyl derivatives, which are much more viscous than the *n*-butyl derivative and the base oils, did not perform as well in the AW test. The *n*-butyl is the least polar and the most soluble of the three derivatives; however, it may provide a potentially less corrosive-wear property to the lubricant.

The evaluation of the AW properties of phosphonylated limonene derivatives as additives in PAO6 and HOSuO base oils is compared in Fig. 8. It should be noted that the three derivatives have similar P content but differ in their viscosity and solubility in base oils. The modified oils lowered both friction and wear at low concentrations from the value of the neat base oils. It is also observed that the improvements are greatest in the base oils where the solubility is the highest. Phosphorous-containing additives are well known to provide AW properties [22], and it appears that the modified limonene derivatives have demonstrated such AW property. In addition, improved compatibility between the polar phosphonate additives and the biobased base oil (HOSuO) has resulted in improved friction and wear performance. Such synergism between biobased base oils and commercial EP additives that resulted in several fold improvements in EP weld point have been reported [5].

4 Summary/Conclusion

Limonene is a natural oil commercially obtained from the processing of citrus fruit byproducts. It is a C10 hydrocarbon with cyclic branching, double bonds, and a chiral carbon in its structure. Limonene is relatively inert at mild temperatures and is used in many applications with or without further structural modifications.

Limonene was chemically modified via a free radical thermal reaction with dialkyl phosphites in the presence of various free radical initiators. Methyl, ethyl, and *n*-butyl phosphites were used, producing mixtures of mono- and bisphosphonate products, which correspond to the addition of the dialkyl phosphite to only one or to both double bonds. The mono- and di-adduct products were identified by a combination of GC–MS, FTIR, and NMR (^{1}H, ^{13}C, ^{31}P) spectroscopies.

The reaction conditions (initiator type, reaction time, etc.) were optimized to produce a high yield of the di-adduct product. The limonene bisphosphonates products with different alkyl substituents on the P were investigated for their physical and tribological properties.

Relative to limonene, the bisphosphonate derivatives displayed the following physical property changes:

- Increased density and viscosity which was attributed to increased polarity in the modified structures resulting in increased intermolecular interactions. The presence of heavy elements (from PO_3) in the modified products was considered a contributor to the increase in density.
- Reduced VI and solubility in the base oils, PAO6 and HOSuO, which was attributed to increased polarity of the modified products.
- Increased oxidation stability, which was attributed to elimination of the double bonds in limonene as a result of the chemical modification.

The tribological properties of limonene bisphosphonates were investigated as neat and also as additives blended into the base oils (PAO6 and HOSuO) on a four-ball tribometer, under AW and EP configurations.

AW investigation of neat limonene bisphosphonates showed COF and WSD that was:

- inferior to values for the base oils (PAO6 and HOSuO) for the ethyl and methyl derivatives
- superior to the base oils for the *n*-butyl bisphosphonate derivatives.

EP investigations of neat limonene bisphosphonates gave weld point values that were slightly higher than that for the base oils.

AW investigation of limonene bisphosphonates as additives in base oils (PAO6 and HOSuO) on a four-ball tribometer showed COF and WSD that were:

- lower than that for the neat base oils
- much lower in the biobased (HOSuO) than in the petroleum-based (PAO6) base oil
- improvement in WSD was attributed to the P in the modified product; P-containing additives are well known to provide EP and AW properties to lubricant formulations.

Chemical modification of limonene through the addition of dialkyl phosphites into its two double bonds has provided access to lubricating oils with: wider density and viscosity range; highly improved oxidation stability; improved EP properties; and improved AW additive properties. The modification has also caused slight reductions in VI and solubility in base oils. Future work is aimed at developing chemical modifications that maximize beneficial properties and minimize negative properties of the modified products.

Acknowledgments The authors are grateful to Dr. Karl Vermillion for the NMR spectra, Ben Lowery for help with running the GC–MS, and Linda Cao for physical and tribological evaluations.

References

1. Bremmer, B.J., Plonsker, L.: Bio-based lubricants: A market opportunity study update. Omni-Tech International, Midland (2008)
2. Schneider, M.P.: Plant-oil-based lubricants and hydraulic fluids. J. Sci. Food Agric. **86**, 1769–1780 (2006)
3. McManus, M.C., Hammond, G.P., Burrows, C.R.: Life-cycle assessment of mineral and rapeseed oil in mobile hydraulic systems. J. Ind. Ecol. **7**(3–4), 163–177 (2003)
4. Lawate, S.S., Lal, K., Huang, C.: Vegetable oils—structure and performance. In: Booser, E.R. (ed.) Tribology Data Handbook, pp. 103–116. CRC Press, New York, NY (1997)
5. Asadauskas, S.J., Biresaw, G., McClure, T.G.: Effects of chlorinated paraffin and ZDDP concentrations on boundary lubrication properties of mineral and soybean oils. Tribol. Lett. **37**(2), 111–121 (2010)
6. Hope, K., Garmier, B.: High performance engine oils with vegetable oil and PAO blends. Society of Tribologists and Lubrication Engineers Annual Meeting and Exhibition. p. 180 (2008)
7. Adhvaryu, A., Biresaw, G., Sharma, B.K., Erhan, S.Z.: Friction behavior of some seed oils: bio-based lubricant applications. Ind. Eng. Chem. Res. **45**(10), 3735–3740 (2006)
8. Biresaw, G., Bantchev, G.: Elastohydrodynamic (EHD) traction properties of seed oils. Tribol. Trans. **53**(4), 573–583 (2010)
9. Erhan, S. Z.: Oxidative stability of mid-oleic soybean oil: Synergistic effect of antioxidant- antiwear additives. In: Proceedings of the USB Lube TAP, Detroit, MI, Oct 24–25, (2006)
10. Honary, L.A.T.: Biobased greases and lubricants: From research to commercialization. In: Proceedings of the USB Lube TAP, (2007)
11. Isbell, T.A.: U.S. effort in the development of new crops (lesquerella, pennycress, coriander and cuphea). Ol. Corps Gras Lipides **16**, 205–210 (2009)
12. Cermak, S.C., Biresaw, G., Murray, R.: New crop oils—properties as potential lubricants. Ind. Crops Prod. **44**, 232–239 (2013)
13. Isbell, T.A., Abbott, T.P., Asadauskas, S., Lohr, J.E., Jr.: Biodegradable Oleic Estolide Ester Base Stocks and Lubricants. U.S. Pat. No. 6,018,063 (2000)
14. Ngo, H.L., Hoh, E., Foglia, T.A.: Improved synthesis and characterization of saturated branched-chain fatty acid isomers. Eur. J. Lipid Sci. Technol. **114**(2), 213–221 (2012)
15. Bantchev, G.B., Kenar, J.A., Biresaw, G., Han, M.G.: Free radical addition of butanethiol to vegetable oil double bonds. J. Agric. Food Chem. **57**(4), 1282–1290 (2009)
16. Adhvaryu, A., Erhan, S.Z., Perez, J.M.: Tribological studies of thermally and chemically modified vegetable oils for use as environmentally friendly lubricants. Wear **257**(3–4), 359–367 (2004)
17. Arca, M.: Oxidative Properties and Thermal Polymerization of Soybean Oil and Application in Gear Lubricants. M.S. Thesis, Pennsylvania State University, University Park, PA (2011)
18. Laszlo, J.A., Compton, D.L., Evans, K.O.: Vegetable oil esterified lipoic acid. U.S. Pat. No. 8,455,666 (2013)
19. Challener, C.: Green lubricants continue progress. *ICIS Chemical Business*, February 23, pp. 201–224 (2014)
20. Mookherjee, B.D., Wilson, R.A.: Essential oils. In: Jacqueline, I., Kroschwitz, J.I., Howe-Grant, M., Humphreys, L., Altieri, L., Lee, J. (eds.) Encyclopedia of Chemical Technology, vol. 17, 4th edn, pp. 603–647. Wiley, New York (1996)
21. Mann, J., Davidson, R.S., Hobbs, J.B., Banthorpe, D.V., Harborne, J.B.: Natural Products: Their Chemistry and Biological Significance. Longman, Essex (1996)
22. Schey, J.A.: Tribology in Metalworking Friction Lubrication and Wear. American Society of Metals, Metals Park, OH (1983)
23. Walsh, M.: Challenges impacting the North American orange oil industry. In: Proceedings of IFEAT International Conference, Montreal, 28 Sept.–3 Oct., pp. 115–122 (2008)
24. Navarro, V.O.: The citrus processing and byproduct industry in Argentina. International Citrus and Beverage Conference, September 15–18, Clearwater Beach, FL (2009)
25. Domb, A.J., Wolnerman, J.S.: Double-layered bioadhesive tables for the topical treatment of oral mucosal disorders. PCT Int. Appl., WO 2009013562 A2 20090129, (2009)
26. Wang, S., Wang, Z.: Charging care agent for vehicle motor. CN 101,007,979 A 20070801, (2007)
27. Alvarez, A.A.: Pharmaceutical formulations, which are solid, in solution, suspension and emulsion containing ranitidine and cisapride. Mex. Pat. Appl., MX 2003012049 A 20050623, (2005)
28. Itoh, M., Hamada, K.: Cleaning solvent containing ethanol and limonene for removing mold deposits. PCT Int. Appl. WO 2002047883 A1 20020620 (2002)
29. Ford, W.G.F., Gardner, T.R.: Solvent compositions for cleaning pipes in oil and gas wells. Can. Pat. Appl. CA 2,154,043 A1 19960119 (1996)
30. Ford, W.G.F., Gardner, T.R.: Solvent compositions for removing pipe dopes, thread lubricants, and the like from metal surfaces. U.S. Pat No. 5,489,394 A (1996)
31. Morikawa, T., Isaka, Y., Ogawa, T., Fujii, S., Tabuchi, Y., Katayama, M.: Aqueous environment-friendly cleaning compositions containing terpenes for cleaning molded plastics. Jpn. Kokai Tokkyo Koho JP 07,278,589 A 19951024 (1995)
32. Hamilton, C.R., Gustafson, R.M.: Process and terpene-containing aqueous composition for cleaning. PCT Int. Appl. WO 9,325,653 A1 (1993)
33. Bayer, I.S., Steele, A., Martorana, P., Loth, E., Robinson, S.J., Stevenson, D.: Biolubricant induced phase inversion and superhydrophobicity in rubber-toughened biopolymer/organoclay nanocomposites. Appl. Phys. Lett. **95**, 063702 (2009)

34. Adams, E.K.: Downhole well lubricant for release of stuck coiled tubing by formation of greasy lubricating emulsion upon rubbing. U.S. Pat No. 5,700,767 A (1997)
35. Coffey, G.L., Coffey, B.H.: Nontoxic and biodegradable lubricant composition. U.S. Pat No. 5,691,285 A (1997)
36. Schulz, H.E.: Penetrating oils. U.S. Pat No. 2,491,774 (1949)
37. Kinnaird, M.G.: Protective coating compositions containing natural materials such as gilsonite and d-limonene for metals, and method of use thereof. U.S. Pat. Appl. 20020114894 A1 20020822 (2002)
38. Leung, D.W.-Y.: Anhydrous composition for protecting, polishing, disinfecting, degreasing, deodorizing, lubricating and cleaning furniture and other surfaces. Can. Pat. Appl. CA 2,187,552 A1 19980409 (1998)
39. Goldblatt, L.A., Oldroyd, D.M.: Halogenated terpene addition compounds. U.S. Pat. No. 2,564,685 (1951)
40. Walsh, R.H.: Sulfurized compositions and lubricants containing them. U.S. Pat No. 4,584,113 A (1986)
41. Oberright, E.A., Leonardi, S.J.: Lubricating oil additives. FR 1,399,146 (1965)
42. Cyphers, E.B., Waddy, W.E.: Oil additive. U.S. Pat No 2,815,326 (1957)
43. Greenwood, J., Jensen, H.C.H.: Sulfurized terpenes for lubricating-oil additives. GB **761**, 579 (1956)
44. Fields, E.K.: Corrosion inhibitors for lubricants for silver and silver alloys. U.S. Pat No. 2,764,547 (1956)
45. Watson, R.W.: Sulfurizing terpenes. U.S. Pat No. 2,445,983 (1948)
46. Fox, A.L.: Metal mercaptides of terpene compounds. U.S. Pat No. 2,407,266 (1946)
47. Fox, A.L.: Metal mercaptides of terpene compounds. U.S. Pat No. 2,407,265 (1946)
48. Fox, A.L.: Copper compounds of mercaptans derived from monocyclic or bicyclic terpenes. GB **580**, 366 (1946)
49. Cizek, J., Rabl, V., Mostecky, J.: Extreme pressure [lubricant] additives. Sbornik Vysoke Skoly Chemicko-Technologicke v Praze, D: Technologie Paliv **6**, 147–161 (1964)
50. Augustine, F.B.: Esters of dithiophosphoric acids and terpenes. U.S. Pat No. 2,665,295 (1954)
51. Hook, E.O., Beegle, L.C.: *S*-(Sulfurized terpene hydrocarbon) dithiophosphoric acid triesters as antioxidants and corrosion inhibitors. U.S. Pat No. 2,657,900 (1953)
52. Kirshenbaum, A.D., Rudel, H.W.: A monocyclic terpene-sulfur-phosphorus sulfide reaction product used as an additive for lubricating oil. U.S. Pat No. 2,654,711 (1953)
53. Cyphers, E.B., Michaels, A.E.: Sulfurized monocyclic terpenes as lubricating-oil additives. U.S. Pat No. 2,654,712 (1953)
54. Hook, E.O., Beegle, L.C.: Esters of dithiophosphoric acid containing terpene radicals. U.S. Pat No. 2,627,523 (1953)
55. Kirshenbaum, A.D., Boyle, J.M.: Sulfurized additives for lubricating compositions. U.S. Pat No. 2,613,183 (1952)
56. Augustine, F.B.: Lubricating-oil additives. U.S. Pat No 2,561,773 (1951)
57. Ott, E.: Terpene reaction product. U.S. Pat No. 2,413,648 (1946)
58. Sheppard, C.S., Kamath, V.R.: The selection and use of free radical initiators. Polym. Eng. Sci. **19**(9), 597–606 (1979)
59. Anon.: Standard practice for calculating viscosity index from kinematic viscosity at 40 and 100 °C. ASTM D 2270-93. 05.01, pp 769–774(2002)
60. Biresaw, G., Laszlo, J.A., Evans, K.O., Compton, D.L., Bantchev, G.B.: Synthesis and tribological investigation of lipoyl glycerides. J. Agric. Food Chem. **62**(10), 2233–2243 (2014)
61. Biresaw, G., Bantchev, G.B.: Tribological properties of biobased phosphonate derivatives. J. Am. Oil Chem. Soc. **90**(6), 891–902 (2013)
62. Anon.: Standard test method for wear preventive characteristics of lubricating fluid (Four-Ball Method). ASTM D 4172-94. 05.02, pp 752–756 (2002)
63. Anon.: Standard test method for determination of the coefficient of friction of lubricants using the Four-Ball wear test machine. ASTM D 5183-95. 05.03, pp 165–169. (2002)
64. Anon.: Standard test method for measurement of extreme-pressure properties of lubricating fluids (Four-Ball Method). ASTM D 2783-88. 05.02, pp 130–137 (2002)
65. Silverstein, R.M., Webster, F.X., Kiemle, D.J.: Spectrometric Identification of Organic Compounds, 7th edn. Wiley, Hoboken, NJ (2005)
66. Bantchev, G.B., Biresaw, G., Vermillion, K.E., Appell, M.: Synthesis and spectral characterization of methyl 9(10)-dialkylphosphonostearates. Spectrochim. Acta A Mol. Biomol. Spectrosc. **110**, 81–91 (2013)
67. Troev, K.D.: Chemistry and Application of H-Phosphonates. Elsevier B. V, Amsterdam (2006)
68. Clara, R.A., Marigliano, A.C.G., Solimo, H.N.: Density, viscosity, and refractive index in the range (283.15 to 353.15) K and vapor pressure of α-Pinene, d-Limonene, (±)-Linalool, and Citral over the pressure range 1.0 kPa atmospheric pressure. J. Chem. Eng. Data **54**(3), 1087–1090 (2009)
69. Harry-O'kuru, R.E., Biresaw, G., Cermak, S.C., Gordon, S.H., Vermillion, K.: Investigation of some characteristics of polyhydroxy milkweed triglycerides and their acylated derivatives in relation to lubricity. J Agric. Food Chem **59**(9), 4725–4735 (2011)